Topography and physiology of ascending streams in the auditory tectothalamic pathway

Charles C. Lee[1] and S. Murray Sherman

Department of Neurobiology, University of Chicago, Chicago, IL 60637

Edited by Michael M. Merzenich, University of California, San Francisco, CA, and approved November 9, 2009 (received for review July 15, 2009)

Auditory information is relayed from the cochlea along parallel pathways and reaches the inferior colliculus (IC) and the medial geniculate body (MGB) en route to the cortex. Although the ascending tectothalamic pathway to the ventral division of the MGB is regarded as a high-fidelity information-bearing channel, the roles of the pathways to the dorsal and medial divisions are more opaque. Here, we show fundamental differences between these ascending pathways using an in vitro slice preparation. Using photostimulation, we found three main patterns of input (excitatory, inhibitory, and mixed) that differed in each pathway. Furthermore, electrical stimulation of the central nucleus of the IC evoked a depressing response in the MGB with no metabotropic glutamate (mGlu) receptor component, whereas stimulation of the lateral cortex of the IC evoked a facilitating response with an mGlu receptor component. These data suggest that the ascending tectothalamic pathways are functionally distinct from one another.

inferior colliculus | thalamus | drivers | modulators | photostimulation

Auditory information ascends from the sensory periphery along parallel pathways, synapsing in the inferior colliculus (IC) and then the medial geniculate body (MGB) en route to the cortex. At the tectothalamic synapse, the IC central nucleus (ICc) reliably transmits excitatory and inhibitory information to the ventral division of the MGB (MGBv) (1, 2). However, the role of the tectothalamic projections from the lateral (ICl), dorsal (ICd), and caudal cortices of the IC [collectively referred to here as the shell region (ICs)] to the dorsal (MGBd) and medial (MGBm) divisions of the MGB are less well understood and may serve either a driving or modulatory role, or both (3, 4). Based on the presence or absence of a cortical layer 5 input, these MGB divisions have been termed first order (MGBv; no layer 5 input) or higher order (MGBd and MGBm; having a layer 5 input), and it is thought that the higher order nuclei play an important role as part of corticothalamocortical circuits (5–7). Previous work in the somatosensory thalamus suggests that the principal driving input to higher order thalamic nuclei arises from this layer 5 input (8). In the auditory system, the anatomical substrates supporting such a driving corticothalamic pathway from layer 5 are also present (6, 7). However, if the cortex provides the principal driving input to the higher order nuclei of the MGB, what is the role of the ascending tectal inputs?

Another issue of interest is the observation that auditory tectothalamic inputs are composed of both excitatory and inhibitory pathways. Anatomical studies suggest that the inhibitory feedforward projections to the MGB arise throughout the IC (9, 10), and physiological investigations find several distinct classes of excitatory and inhibitory inputs (11–13). However, the topographic organization of excitatory and inhibitory inputs in the tectothalamic pathways is largely undefined. Are these pathways organized similarly across collicular and thalamic nuclei? Do they align topographically with the anisotropic frequency organization in the ICc and MGBv (1, 2)? Do excitatory and inhibitory inputs arise from the same loci, or are they topographically segregated?

To investigate these issues of auditory tectothalamic organization, we developed an in vitro tectothalamic slice preparation in the mouse containing parts of the ascending pathways to the MGB. Whole-cell recordings of MGB neurons in response to photostimulation in the IC with caged glutamate were used to map the topography of excitatory and inhibitory inputs and to identify loci for subsequent electrical stimulation as well as to identify these tectothalamic synaptic inputs as drivers or modulators (5, 8, 12).

Results

Slice Preparation. To investigate the topographic and synaptic properties of the tectothalamic pathways, we developed a unique in vitro slice preparation that preserved parts of the pathways from the IC to the MGB (Fig. 1). This was based on analysis of the gross anatomical organization of the tectothalamic pathway in the mouse, which led to a slice preparation angled 35° up dorsocaudally from the horizontal plane of section (14) (see *Materials and Methods*; Fig. 1*C*). To verify that intact connections were preserved in the slice, biocytin was iontophoresed in the IC of physiologically connected slices ($n = 6$) (Fig. 1 *A–D*). Labeled fibers traversed from the IC along the brachium of the IC and terminated in the MGB (Fig. 1 *B* and *D*).

Cytoarchitectonic staining (Nissl and parvalbumin immunohistochemistry) revealed that multiple collicular subdivisions (ICc, ICl, and ICd) and thalamic nuclei (MGBv, MGBd, and MGBm) were present in the slice plane (Fig. 1 *E* and *F*). In material stained with cresyl violet (Fig. 1*E*) or thionin (Fig. S1*B*), the laminated structure of the MGBv could be discerned from the more diffuse organization of the MGBd or MGBm (Fig. S1*B*). MGBv neurons were also smaller and more tightly packed than neurons in the MGBd and, particularly, the MGBm (2) (Fig. S1*B*). Although less obvious in the living slice preparation, these cytoarchitectonic features could often be discerned under differential interference contrast (DIC) optics (Fig. S1*A*). The angle of the slice situated the MGBd caudal and somewhat lateral to the MGBv in the final slice plane (Fig. 1 *E* and *F* and Fig. S1 *B* and *C*). Parvalbumin stained the ICc and MGBv more intensely than the surrounding structures (15, 16) (Fig. 1*F* and Fig. S1 *C* and *F*). The ICc was particularly visible in parvalbumin-stained sections as an intensely stained tear-shaped region surrounded by the more lightly stained ICl and ICd, which we collectively refer to as the ICs (Fig. 1*F* and Fig. S1*F*). This subdivision geometry in the slice was also visible in Nissl-stained material (Figs. 1*E* and 2*E*) and in the living slice under DIC optics (Fig. S1*D*), which readily enabled the identification of subregions during physiological recordings. Intact projections in the slice were further verified using photostimulation (17–19), which was found to activate spiking only in IC neurons within ~100 μm of the soma (ICc: $n = 5$, ICl: $n = 5$) (Fig. S2), validating the specificity of photostimulation in the IC.

Author contributions: C.C.L. and S.M.S. designed research; C.C.L. performed research; C.C.L. and S.M.S. analyzed data; and C.C.L. and S.M.S. wrote the paper.

The authors declare no conflict of interest.

This article is a PNAS Direct Submission.

[1]To whom correspondence should be addressed at: Department of Neurobiology, University of Chicago, 947 East 58th Street, MC 0926, Chicago, IL 60637. E-mail: clee@bsd.uchicago.edu.

This article contains supporting information online at www.pnas.org/cgi/content/full/0907873107/DCSupplemental.

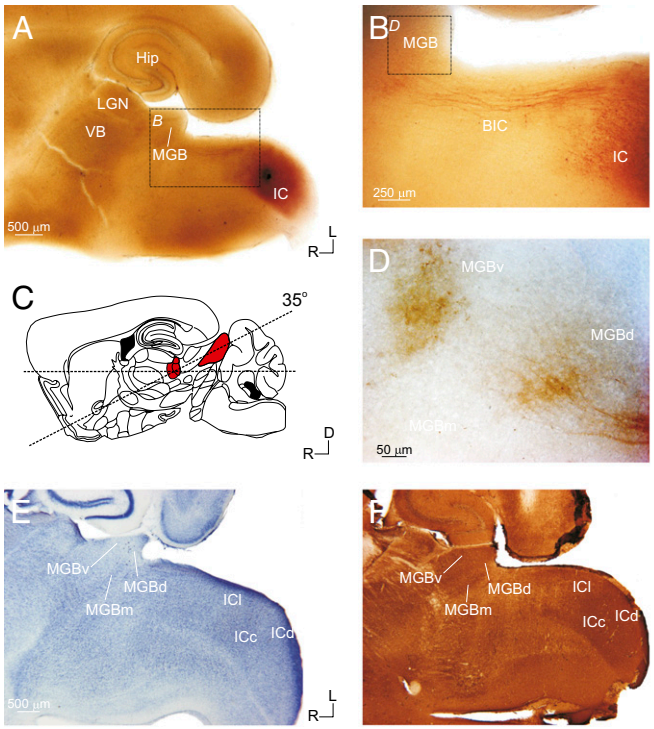

Fig. 1. Anatomical and histological characterization of the auditory tectothalamic slice. The slice was prepared with a 35° blocking cut on the dorsal surface (*C*; red-shaded areas indicate the MGB and IC, respectively) [adapted from Paxinos and Franklin (14)]. Biocytin injections in the IC of the slice (*A*) labeled tectothalamic fibers, which traversed through the brachium of the inferior colliculus (BIC) (*B*) and terminated in the MGB (*D*). Nissl (*E*) and parvalbumin (*F*) staining delineated the IC and MGB subdivisions. (Scale bars: *A*, 500 μm; *B*, 250 μm; *D*, 50 μm.)

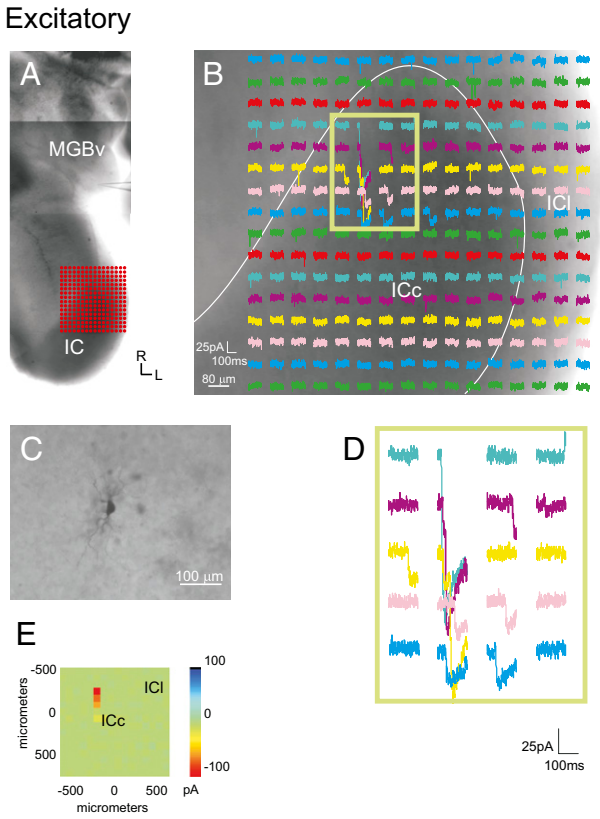

Fig. 2. Photostimulation of the IC elicits excitatory responses in the MGB. (*A*) Recording locations in the MGB and the photostimulation sites in the IC, as shown in a photomontage of the slice. Grid of 16 × 16 dots indicates the stimulation sites as depicted in *B*. (*B*) Photostimulation response map in the IC. Each trace depicts the response of the recorded MGB neuron to photostimulation at each IC site. (*C*) Recorded bitufted MGB neuron labeled with biocytin. (*D*) Higher magnification traces of boxed region. (*E*) Mean amplitude of photostimulation responses. (Scale bars: *B*, 80 μm; *C*, 100 μm.)

Photostimulation. To validate the tectothalamic slice preparation further and to assay the topographic organization of ascending excitatory and inhibitory inputs, the responses of MGB neurons to photostimulation of the IC were recorded. In each experiment (n = 24), a Cs^+ solution in the recording pipette (see *Materials and Methods*) was used to hold the neuron at depolarized potentials (~0 to −10 mV) to enable the clear visualization of both excitatory postsynaptic currents (EPSCs) and inhibitory postsynaptic currents (IPSCs). A stimulation grid was then oriented over the IC (16 ×16, 80-μm spacing), and traces were recorded for 150 ms following the laser-mediated photolysis of the caged-glutamate compound (Figs. 2–5 and Fig. S3). MGB neurons responded robustly to photostimulation of the IC (Figs. 2–5 and Fig. S3). This further validated that intact projections are present in the slice preparation.

In control experiments, photostimulation was found to activate neurons in the IC only within ~100 μm of the cell body or proximal dendrites (Fig. S2). This was found to be the case for neurons in both the ICc (Fig. S2 *A–C*) and ICl (Fig. S2 *D–F*). At distances slightly greater than 100 μm, slight depolarizations were sometimes observed that did not result in spiking. In addition, stimulation of the ICc did not result in spiking of ICl neurons (20), suggesting that the intrinsic collicular projections are either not intact in this slice plane or are not sufficiently robust to exceed threshold. These results validated the specificity of stimulation via glutamate uncaging (17–19).

In our survey of the topographic patterns of tectothalamic inputs, we found three patterns of convergent inputs to MGB neurons: excitatory, inhibitory, and mixed (both excitatory and inhibitory) (Figs. 2–5 and Fig. S3). Neurons that responded only to excitatory IC stimulation (n = 6) (Fig. 2) resided wholly in the MGBv and had bitufted morphologies (n = 4) (Fig. 2*C*). The main excitatory response regions arose exclusively from the ICc and were generally very large in amplitude (~100 pA) (Fig. 2*B* and Table 1). The excitatory input maps often extended over large regions (>500 μm), suggesting high excitatory convergence onto a single neuron (Fig. 2*D*). No neurons receiving purely excitatory inputs were found in the MGBd, and no neuron received purely excitatory input from the ICl.

In contrast, purely inhibitory MGB responses (n = 5) resulted from photostimulation of both the ICc and ICl, although ICl inhibition was often stronger (~80 pA) and more highly clustered (Figs. 3 and 5, Fig. S3, and Table 1). Unlike the excitatory inputs to the MGB, inhibitory inputs generally originated from multiple IC domains and also covered a large area within the IC (Figs. 3 and 5 and Fig. S3, cell 1). These neurons receiving inhibitory

Table 1. Average response amplitudes (pA) elicited by IC photostimulation

	ICc	ICs*
Excitatory	93.1 ± 21.0	N/A
Inhibitory	29.3 ± 5.8	78.6 ± 19.9
Mixed excitatory	24.2 ± 6.1	20.1 ± 4.1
Mixed inhibitory	17.5 ± 7.4	37.3 ± 8.2

*Includes ICl and ICd.

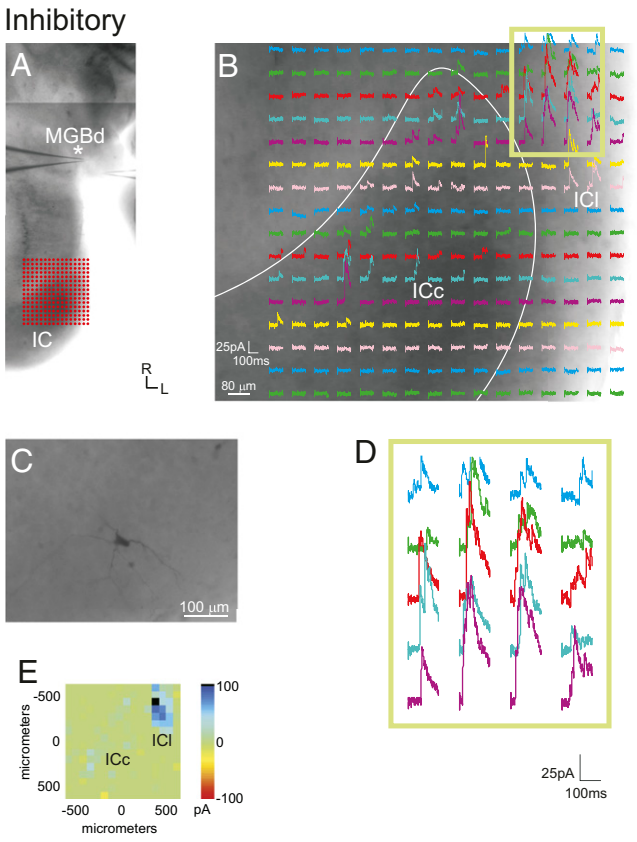

Fig. 3. Inhibitory responses elicited in the MGB following photostimulation of the IC. (*A*) Location of patch recordings (asterisk indicates the recorded neuron) and photostimulation sites, as shown in a photomontage of the slice. (*B*) MGB response maps to IC photostimulation. Location of the stimulation grid is shown in *A*. (*C*) Biocytin-filled stellate neuron in the MGB. (*D*) Higher magnification traces from boxed region in *B*. (*E*) Mean amplitude of photostimulation responses. (Scale bars: *B*, 80 μm; *C*, 100 μm.)

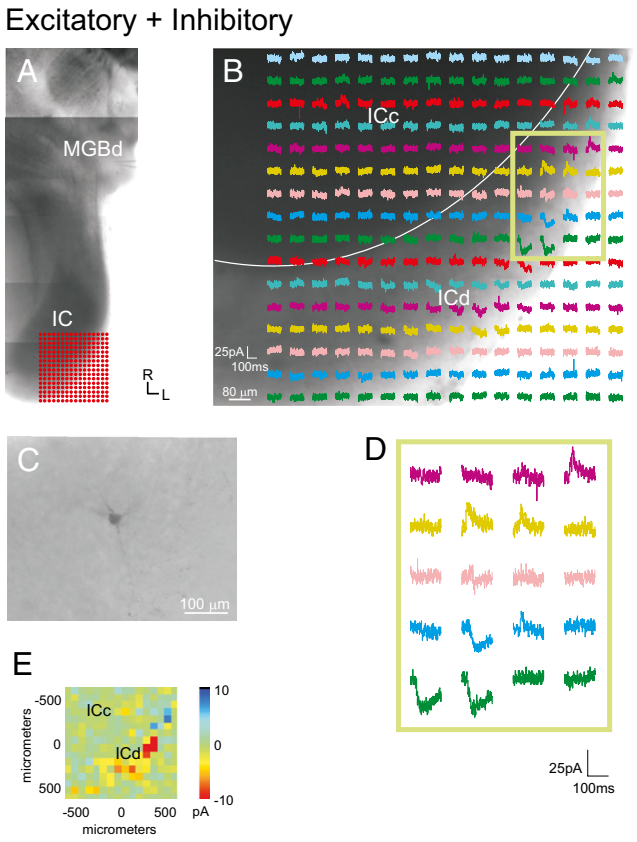

Fig. 4. Mixed excitatory and inhibitory responses following photostimulation of the IC. (*A*) Photostimulation sites in the IC and recording locations, as shown in a photomontage of the slice. Grid in IC indicates photostimulation sites in *B*. (*B*) Responses of the MGB neuron following photostimulation of the IC. (*C*) Recorded stellate MGB neuron labeled with biocytin. (*D*) Traces in boxed region in *B* at higher magnification. (*E*) Mean amplitude of photostimulation responses. (Scale bars: *B*, 80 μm; *C*, 100 μm.)

inputs had both bitufted ($n = 2$) and stellate ($n = 3$) morphologies, and they were found primarily in the MGBd ($n = 4$).

Mixed inputs ($n = 13$) targeting the MGBd ($n = 8$) originated from the ICl ($n = 4$), ICd ($n = 2$), and, in some instances, both the ICc and ICl ($n = 2$) (Figs. 4 and 5 and Fig. S3, cell 2), and they targeted primarily stellate neurons ($n = 8$). The mixed inputs to the MGBv originated from the ICc ($n = 3$) or both the ICc and ICl ($n = 2$). The sizes of both EPSCs and IPSCs were generally smaller than those elicited from purely inhibitory or excitatory inputs (~20 pA) (Fig. 3 and Table 1). In all cases with mixed inputs, the loci of excitatory and inhibitory inputs were topographically segregated within a subdivision (Fig. 3*B*) and were particularly marked when mixed inputs originated from both subdivisions (Figs. 3 and 5 and Fig. S3).

The topographic distributions of excitatory and inhibitory IC inputs to the MGB were assessed with two metrics: anisotropy and convergence. An anisotropy index was used to compare the lengths of the major and minor axes of the IC projection zones (Fig. S4*A*), because neurons in both the MGBv and ICc have previously been shown to be organized anisotropically along isofrequency laminae (1, 2). Interestingly, excitatory and inhibitory inputs from both the ICc and ICl showed statistically similar levels of anisotropy (Fig. S4*B*) ($P > 0.05$, ANOVA; excitatory ICc: 0.72 ± 0.16, excitatory ICl: 0.83 ± 0.14, inhibitory ICc: 0.84 ± 0.12, inhibitory ICl: 0.76 ± 0.13). In addition, topographic convergence was computed for the experiments in which dual MGB recordings were performed simultaneously ($n = 5$) (e.g., Fig. 5 and Fig. S3). The distance between recording sites was compared with the distance between the centers of the main excitatory ($n = 3$ of 5) and inhibitory ($n = 5$ of 5) projection sources in the IC (Fig. S4*C*). In each experiment, the separation of IC projection sources was greater than that predicted from a linear correspondence with the MGB recording sites, indicating a large degree of tectothalamic convergence (Fig. S4*D*).

Pharmacology. To characterize pharmacologically the ascending inhibitory inputs and to determine whether masked excitatory inputs originated from the same loci, pharmacological blockers of GABA receptors (SR 95531: 20 μM for $GABA_A$, CGP 46381: 40 μM for $GABA_B$) were added to the bath after the initial topographic mapping described above ($n = 15$ of 24) (Fig. 5 and Fig. S3). In all cases, $GABA_A$ receptor blockers abolished the inhibitory response (Fig. 5 *B* and *C*, *Middle*, and Fig. S3 *B* and *E*). Furthermore, GABA receptor blockade did not reveal any weaker masked excitatory inputs originating from the same loci as the inhibitory inputs, suggesting that ascending inhibitory and excitatory inputs originate from topographically separate IC loci.

Interestingly, in all experiments ($n = 15$), blockade of $GABA_A$ receptors resulted in the unmasking of a pronounced excitatory response that originated from the central portion of the ICc, and the topographic origin of this response was highly consistent across experiments (Fig. 5 *B* and *C*, *Middle*, and Fig. S3 *B* and *E*). This induced excitatory response was sensitive to NMDA receptor blockers (MK-801, 40 μM) (Fig. 5 *B* and *C*, *Right*, and

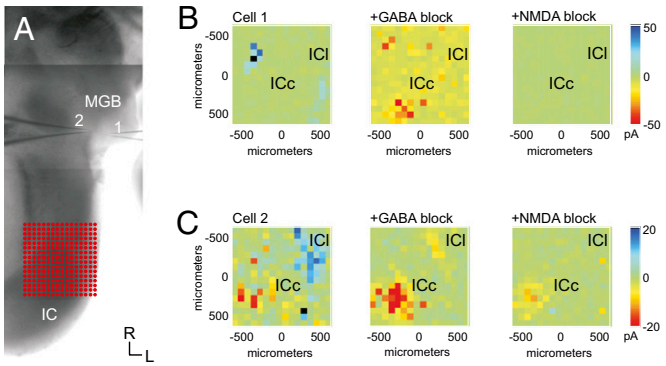

Fig. 5. Pharmacology of the tectothalamic response. Blocking inhibitory IC input reveals a robust NMDA current elicited from the ICc. (*A*) In this experiment, two MGB neurons were recorded simultaneously in response to photostimulation in the IC, as shown in a photomontage of the slice. (*B* and *C*) Mean evoked currents. Traces are shown in Fig. S3. Cell 1 received robust inhibitory input from the external shell of the IC (ICs), whereas cell 2 received both inhibitory ICs input and excitatory ICc input (*Left*). Bath application of GABA receptor antagonists eliminates the IPSCs, while revealing large EPSCs in the ICc (*Center*). These large EPSCs are eliminated following bath application of NMDA antagonists, leaving the AMPA-mediated EPSCs in cell 2 unaffected (*Right*).

Fig. S3 *C* and *F*) but was insensitive to type 1 mGlu receptor blockers (S4CPG, 80 μM).

Electrical Stimulation. To examine the synaptic effects of paired-pulse and high-frequency stimulation, we recorded from MGB neurons (n = 15) in either the ICc-to-MGBv pathway (n = 7) or the ICl-to-MGBd pathway (n = 8), using a normal intracellular solution. These neurons had an average resting potential of −63.2 ± 2.7 mV and an average input resistance of 238.1 ± 63.2 MΩ. No significant difference ($P < 0.05$, t test) was found in resting potentials between MGBv (−61.7 ± 2.1 mV) and MGBd (−64.4 ± 2.7 mV) neurons. Hyperpolarizing and depolarizing current injections were used to characterize recorded neurons (Fig. 6 *B* and *F*). Hyperpolarizing current injections were found to induce burst (postinhibitory rebound) spiking in both neuron types and also included a prominent hyperpolarization-activated (I_h) current in most MGBv neurons (n = 6 of 7) but rarely in MGBd neurons (n = 2 of 8) (11, 21). Depolarizing currents elicited regular spiking behavior, consistent with previous studies (11, 21).

Photostimulation was used to identify the IC region that elicited responses in the recorded MGB neuron in the presence of NMDA and GABA receptor blockers (MK-801: 40 μM for NMDA, SR 95531: 20 μM for $GABA_A$, CGP 46381: 40 μM for $GABA_B$). A bipolar concentric electrode was then targeted to the IC region that elicited the maximal excitatory responses (Fig. 6 *A* and *E*). In both pathways, latencies of excitatory responses were short with low-onset jitter (ICc to MGBv: 4.94 ± 1.35 ms, ICl to MGBd: 4.68 ± 1.76 ms), indicating monosynaptic responses. In response to paired-pulse stimulation, neurons (n = 7) in the ICc-to-MGBv pathway exhibited depressing EPSPs. This effect was quantified by measuring the ratio of the second EPSP amplitude to that of the first EPSP amplitude (EPSP2/EPSP1). The depressing effect was most pronounced at higher frequencies [40 Hz: paired-pulse ratio (PPR) = 0.59 ± 0.21] (Fig. 6*C* and Table 2). In contrast, MGBd neurons (n = 8) exhibited facilitating EPSPs to ICl stimulation that were most pronounced at higher stimulation frequencies (40 Hz: PPR = 1.26 ± 0.11) (Fig. 6*G* and Table 2). At each frequency, these ratios in each pathway were significantly different from each other ($P < 0.05$, t test).

To determine whether the ascending pathways activate an mGlu response, high-frequency stimulation (125 Hz for 800 ms) was used in the presence of ionotropic glutamate (iGlu) receptor and GABA receptor blockers (DNQX: 50 μM for AMPA, MK-801: 40 μM for NMDA, SR 95531: 20 μM for $GABA_A$, CGP 46381: 40 μM for $GABA_B$). High-frequency stimulation of the ICc-to-MGBv pathway resulted in no long-term responses (Fig. 6*D*). In contrast, neurons in the ICl-to-MGBd pathway exhibited a prominent depolarization (~4 mV) that lasted several hundred milliseconds (Fig. 6*H*). This depolarizing response was abolished in the presence of group 1 mGlu receptor antagonists (S4CPG: 80 μM) (Fig. 6*H*). Thus, these pathways are distinguished by unique synaptic properties: The former shows paired-pulse depression with no mGlu receptor component, whereas the latter shows paired-pulse facilitation with an mGlu receptor component.

Discussion

Tectothalamic Slice Preparation. We examined the topographic organization and synaptic properties of the ascending pathways from the IC to the MGB using a unique in vitro tectothalamic slice preparation. This preparation preserved parts of the pathways from the IC to the MGB, which was verified anatomically and physiologically. Biocytin injections in the IC labeled fibers that terminated in the MGB, and electrical and photostimulation of the IC produced robust excitatory and inhibitory responses in recorded MGB neurons. In particular, photostimulation only results in neuronal activation at the cell body or proximal dendrites (17, 18) (Fig. S2), thus confirming that intact tectothalamic projections were present in the slice.

The delineation of nuclear and subdivision boundaries in the MGB and IC was established using cytoarchitectonic markers, Nissl staining, and parvalbumin immunohistochemistry (2, 15), and the boundaries were visible with DIC optics in the living slice. However, some caution may be warranted with respect to the boundaries established in this manner because their correlation with functional borders established in vivo is tentative (2, 22, 23). In addition, recorded neurons were localized based on a combination of the gross anatomical features, cell morphology, and intrinsic physiology. Each feature by itself is not definitive; however, when used together, they helped to reconstruct nuclear location. Nevertheless, the present parcellation should be considered valid insofar as the observed topography and physiology of both the tectothalamic streams follow a pattern that is compatible with previous anatomical and physiological studies (1, 11, 24).

In addition, much of the collicular input to the MGBd in the slice was found to originate from the ICl, which has previously been shown to innervate the nontonotopic nuclei of the MGB (dorsal, deep dorsal, suprageniculate, ventrolateral) strongly (3). Thus, the present conclusions regarding the tectothalamic inputs to the MGBd are derived primarily from the ICl and, to a lesser extent, the ICd, and thus may not extend generally to the ICs as a whole. The few neurons recorded from the ICd thus pose a potential sampling bias for our broader conclusions related to the organization of the parallel ascending tectothalamic pathways. The ICl also receives weak inputs from the lateral lemniscus, in addition to the nonlemniscal input (1, 3, 25). However, because its primary input does not originate from lemniscal sources, we have considered the ICl input to the MGBd as an input to a higher order thalamic nucleus (see below).

Previous investigations of the auditory tectothalamic pathways used preparations that only preserved the afferent fibers (e.g., brachium of the IC, corticothalamic fibers) to the MGB (9, 11, 13, 24). Despite the lack of intact structures innervating the MGB in these earlier preparations, the parallel organization of the tectothalamic pathways allowed some specificity of responses from fiber stimulation (12, 24). For example, Hu et al. (24) demonstrated that brachial stimulation resulted in burst firing from MGBd neurons predominantly, and Bartlett and Smith (11, 12) demonstrated differential excitatory and inhibitory responses to brachial stimulation in MGBv and MGBd neurons. Our

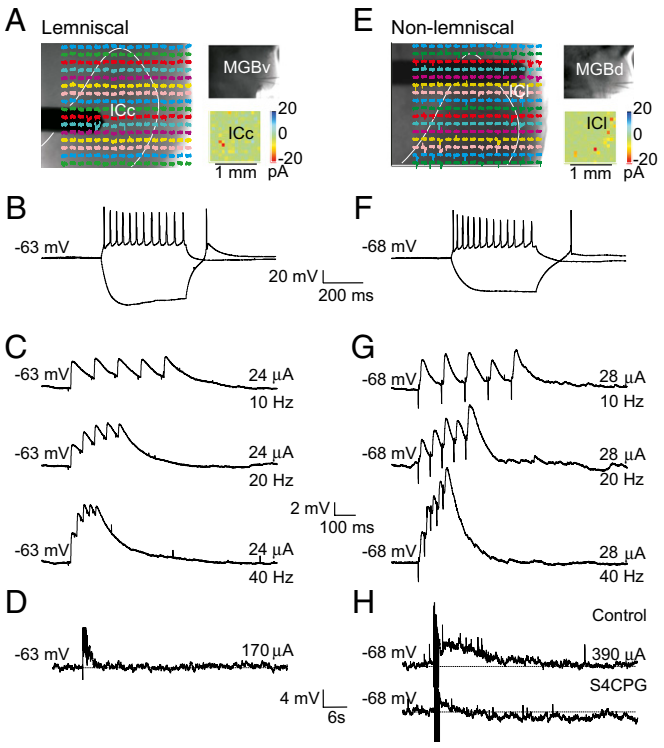

Fig. 6. Electrical stimulation of tectothalamic inputs to the MGBv (*A–D*) and MGBd (*E–G*) pathways. (*A* and *E*) Photostimulation guided the placement of the stimulating electrode. (*B* and *F*) Intrinsic properties of recorded MGB neurons. Most MGBv neurons exhibited a pronounced hyperpolarization-activated (I_h) current. The tectothalamic pathway to MGBd depressed in response to paired pulses (*C*) and showed no mGlu receptor component (*D*), whereas the pathway to MGBd facilitates (*G*) and has a group 1 mGlu receptor response (*H*).

preparation now enables the unambiguous localization of the tectal sources of input to the MGB, which we employed to map inputs topographically using photostimulation and to target IC regions specifically for electrical stimulation, as discussed below.

Topography of Ascending Inputs. Ascending excitatory and inhibitory inputs in the auditory tectothalamic pathway have been identified and characterized in previous studies (9–13, 24). Bartlett and Smith (11, 12) found that mixed excitatory and inhibitory inputs predominate across MGB divisions. Our finding of purely excitatory inputs to the MGBv is consistent with their findings, although they also found purely excitatory inputs to the MGBd, which may not have been maintained in our slice preparation or may be a result of undersampling. Similar to the previous results, we also found that few neurons receive purely inhibitory inputs; however, as demonstrated by our pharmacology results, these neurons also have an excitatory component that is revealed following GABA blockade. As such, these neurons may be more comparable to the large population of mixed inputs that has been described previously (12). Thus, the basic classes of inputs appear to be consistent with previous studies, and the few differences may reflect methodological issues, that is, photostimulation of the IC (present results) and electrical stimulation of the brachium of the IC (12, 24), sampling methodology, or potential species-specific distinctions. In addition, our results extend these previous results by topographically identifying the IC sources of these excitatory and inhibitory inputs to the MGB.

Purely excitatory inputs originate primarily from the ICc, are large in amplitude, are distributed across a large region, and exhibit a high degree of topographic convergence. This pattern of input is consistent with the known functional role of the collicular input to the MGBv, transmitting high-fidelity frequency-specific information from the sensory periphery (4). The excitatory inputs are consistent with the anatomically robust interconnections among frequency-specific laminae in both the IC and MGB (1, 2). However, the pattern is not constrained by a simple point-to-point topography, because IC inputs often extend over a large area and have larger than predicted topographic separations, suggesting a high degree of ascending excitatory convergence.

Purely inhibitory inputs are distributed across large IC regions in all the tectothalamic pathways studied. The widespread origins of the ascending inhibitory pathways suggest that they may play a global role in hyperpolarizing MGB neurons, resulting in a preferential switch to burst-firing mode (26). In this respect, inhibitory inputs originating from the ICl were often found to be stronger than those originating from the ICc, suggesting that MGBd neurons may be hyperpolarized preferentially and prone to low-threshold calcium spiking. Although we found no significant difference in resting potentials in vitro, the situation in vivo may differ, and previous studies suggest that MGBd neurons may rest at more hyperpolarized potentials than MGBv neurons (21, 24). Similar to the excitatory inputs, the inhibitory inputs exhibited a similar level of anisotropy compared with the excitatory inputs and also were separated topographically by a greater degree than predicted.

Mixed excitatory and inhibitory inputs were always found to be topographically segregated and generally smaller in amplitude than purely excitatory and inhibitory inputs. Thus, for this class, the excitatory IC inputs to MGB neurons are inhibited by convergent inputs from neighboring channels, perhaps enabling a sharpening of the receptive field (27). Bartlett and Smith (11, 12) found a similar class of mixed inputs, which were further segregated based on the temporal sequence of excitation and inhibition. Similar fine latency discriminations were largely impractical with photostimulation (17), although electrical stimulation in our study resulted in excitatory latencies that were comparable to those of previous reports (12, 24). It is reasonable to presume that the mixed excitatory and inhibitory patterns observed here also may be further segregated in the temporal domain.

Functional Implications. Our results demonstrate physiological differences in parts of the tectothalamic pathways. For those regions that were connected in our slice, photostimulation of the ICc generally resulted in large EPSCs, weaker IPSCs, and an NMDA-sensitive current that was unmasked following GABA receptor blockade. Stimulation of ICl, however, resulted in smaller EPSCs, larger IPSCs, and no NMDA-sensitive current following GABA receptor blockade. Furthermore, electrical stimulation of the ICc evoked depressing responses, whereas stimulation in the ICl evoked facilitating responses with an mGlu receptor 1 component, which is consistent with and extends previous findings (11, 12, 24).

Interestingly, these physiological characteristics resemble the driver and modulator properties found in the somatosensory thalamus (8) and layer 4 cells in the auditory and somatosensory cortices (28, 29). In this framework, driver inputs are physiologically characterized by large EPSPs, paired-pulse depression, and no mGlu receptor component, whereas modulator inputs demonstrate paired-pulse facilitation and an mGlu receptor component (5). Our data suggest that these criteria also extend to the auditory tectothalamic projection.

In this respect, the ascending pathway to the MGBv exhibits driver properties and is the primary conduit for information ascending to the auditory thalamus, whereas the pathway to the MGBd provides modulatory input instead (Fig. S5). Furthermore, we have previously demonstrated that the thalamo-

Table 2. PPRs in the tectothalamic pathways

	5 Hz	10 Hz	20 Hz	40 Hz
ICc to MGBv	0.82 ± 0.12	0.76 ± 0.21	0.62 ± 0.13	0.59 ± 0.21
ICl to MGBd	1.05 ± 0.19	1.13 ± 0.13	1.21 ± 0.21	1.26 ± 0.11

$P < 0.05$.

cortical projection from both the MGBv and MGBd exhibits driving synaptic properties (28) and the corticothalamic projection from layer 5 of AI to the MGBd has driver-like anatomical features (e.g., large terminals that synapse on proximal dendrites) (6). This potentially establishes an information-bearing route from AI to AII via a corticothalamocortical pathway (5, 30), or perhaps via corticocollicular routes (31).

Previous schemes have suggested that the ascending pathways to the MGBv and MGBd represent parallel paths of information processing (4), but our data support an alternative interpretation. This alternative interpretation is that there is only one main information-processing stream from the periphery, namely, the pathway from the ICc to MGBv, and that the ICl-to-MGBd pathway modulates the higher order processing of the corticothalamocortical pathway through MGBd instead, supporting the importance of such corticothalamocortical routes for higher order processing (5).

In this context, similar considerations might apply to the somatosensory and visual pathways. For the somatosensory system, the prevailing view is that the lemniscal (via the ventral posterolateral nucleus [VPL] and the ventral posteromedial nucleus [VPM]) and nonlemniscal (via the posteromedial complex [POm]) pathways represent parallel information streams (32), but the possibility remains that the nonlemniscal pathways are modulatory instead of information-bearing. Likewise, for the visual system, the nature of the tectothalamic pathway from the superior colliculus to pulvinar needs to be determined: Is it a modulator of corticopulvinar-cortical pathways or a parallel visual pathway, or both? Studies in the cat (33) and monkey (34) suggest that these tectal inputs may instead drive pulvinar neurons, implying that prospective differences exist between the visual and auditory systems, and thus may belie a simple canonical principle for organizing the ascending sensory pathways.

Materials and Methods

Slice Preparation. Tectothalamic slice preparations were made from BALB/c mice (aged 10–16 days). All procedures were approved by the Institutional Animal Care and Use Committee of the University of Chicago. Animals were deeply anesthetized with isoflurane before decapitation. The brains were quickly removed and submerged in cool, oxygenated, artificial cerebral spinal fluid (ACSF; 125 mM NaCl, 25 mM $NaHCO_3$, 3 mM KCl, 1.25 mM NaH_2PO_4, 1 mM $MgCl_2$, 2 mM $CaCl_2$, 25 mM glucose). To prepare the tectothalamic slice, a parasagittal blocking cut was made along the right hemisphere, and the brain was then oriented with this parasagittal surface down. Next, a semihorizontal blocking cut was made along the dorsal surface of the brain tilted 35° dorsocaudally up from the horizontal plane, which preserved the pathway from the IC to the MGB (Fig. 1C). The dorsal surface of this block was then affixed to a vibratome (Campden Instruments) stage in cool ACSF, and slices were cut at 500 μm. This resulted in one viable slice per animal ($n = 55$) that contained intact connectivity between the IC and MGB. Slices were maintained at 32°C in ACSF before being transferred to the recording chamber.

Patch Recording, Anatomy, Pharmacology, and Stimulation. Whole-cell recordings of MGB neurons in response to photostimulation and electrical stimulation, pharmacology, and the histological processing of tissue were carried out using standard procedures, as described in our related studies of cortical synapses (28, 29). For detailed procedures, see *SI Materials and Methods*.

ACKNOWLEDGMENTS. We thank the late J. A. Winer for his comments on an early draft of this manuscript and for his past mentorship and guidance (to C.C.L.). We also thank J. S. Roseman for histology assistance. This work was supported by National Institutes of Health Grants R01DC008794 and R01EY003038 (to S.M.S.) and F32NS054478 (to C.C.L.).

1. Oliver DL, Huerta MF (1992) *Springer Handbook of Auditory Research. The Mammalian Auditory Pathway: Neuroanatomy*, eds Webster DB, Popper AN, Fay RR (Springer, New York), Vol 1, pp 168–221.
2. Winer JA (1992) *Springer Handbook of Auditory Research. The Mammalian Auditory Pathway: Neuroanatomy*, eds Webster DB, Popper AN, Fay RR (Springer, New York), Vol 1, pp 222–409.
3. Wenstrup JJ (2005) *The Inferior Colliculus*, eds Winer JA, Schreiner CE (Springer, New York), pp 200–230.
4. Hu B (2003) Functional organization of lemniscal and nonlemniscal auditory thalamus. *Exp Brain Res* 153:543–549.
5. Sherman SM, Guillery RW (2006) *Exploring the Thalamus and Its Role in Cortical Function* (MIT Press, Cambridge, MA).
6. Llano DA, Sherman SM (2008) Evidence for nonreciprocal organization of the mouse auditory thalamocortical-corticothalamic projection systems. *J Comp Neurol* 507:1209–1227.
7. Winer JA, Larue DT, Huang CL (1999) Two systems of giant axon terminals in the cat medial geniculate body: Convergence of cortical and GABAergic inputs. *J Comp Neurol* 413:181–197.
8. Reichova I, Sherman SM (2004) Somatosensory corticothalamic projections: Distinguishing drivers from modulators. *J Neurophysiol* 92:2185–2197.
9. Peruzzi D, Bartlett EL, Smith PH, Oliver DL (1997) A monosynaptic GABAergic input from the inferior colliculus to the medial geniculate body in rat. *J Neurosci* 17:3766–3777.
10. Winer JA, Saint Marie RL, Larue DT, Oliver DL (1996) GABAergic feedforward projections from the inferior colliculus to the medial geniculate body. *Proc Natl Acad Sci USA* 93:8005–8010.
11. Bartlett EL, Smith PH (1999) Anatomic, intrinsic, and synaptic properties of dorsal and ventral division neurons in rat medial geniculate body. *J Neurophysiol* 81:1999–2016.
12. Bartlett EL, Smith PH (2002) Effects of paired-pulse and repetitive stimulation on neurons in the rat medial geniculate body. *Neuroscience* 113:957–974.
13. Smith PH, Bartlett EL, Kowalkowski A (2007) Cortical and collicular inputs to cells in the rat paralaminar thalamic nuclei adjacent to the medial geniculate body. *J Neurophysiol* 98:681–695.
14. Paxinos G, Franklin KBJ (2001) *The Mouse Brain in Stereotaxic Coordinates* (Academic, New York).
15. Cruikshank SJ, Killackey HP, Metherate R (2001) Parvalbumin and calbindin are differentially distributed within primary and secondary subregions of the mouse auditory forebrain. *Neuroscience* 105:553–569.
16. Chernock ML, Larue DT, Winer JA (2004) A periodic network of neurochemical modules in the inferior colliculus. *Hear Res* 188:12–20.
17. Shepherd GM, Pologruto TA, Svoboda K (2003) Circuit analysis of experience-dependent plasticity in the developing rat barrel cortex. *Neuron* 38:277–289.
18. Lam YW, Sherman SM (2007) Different topography of the reticulothalmic inputs to first- and higher-order somatosensory thalamic relays revealed using photostimulation. *J Neurophysiol* 98:2903–2909.
19. Barbour DL, Callaway EM (2008) Excitatory local connections of superficial neurons in rat auditory cortex. *J Neurosci* 28:11174–11185.
20. Saldaña E, Merchán MA (2005) *The Inferior Colliculus*, eds Winer JA, Schreiner CE (Springer, New York), pp 155–181.
21. Hu B (1995) Cellular basis of temporal synaptic signalling: an in vitro electrophysiological study in rat auditory thalamus. *J Physiol* 483 (pt 1):167–182.
22. Stiebler I, Ehret G (1985) Inferior colliculus of the house mouse. I. A quantitative study of tonotopic organization, frequency representation, and tone-threshold distribution. *J Comp Neurol* 238:65–76.
23. Hage SR, Ehret G (2003) Mapping responses to frequency sweeps and tones in the inferior colliculus of house mice. *Eur J Neurosci* 18:2301–2312.
24. Hu B, Senatorov V, Mooney D (1994) Lemniscal and non-lemniscal synaptic transmission in rat auditory thalamus. *J Physiol (London)* 479:217–231.
25. Loftus WC, Malmierca MS, Bishop DC, Oliver DL (2008) The cytoarchitecture of the inferior colliculus revisited: a common organization of the lateral cortex in rat and cat. *Neuroscience* 154:196–205.
26. Sherman SM (2001) Tonic and burst firing: Dual modes of thalamocortical relay. *Trends Neurosci* 24:122–126.
27. Wu Y, Yan J (2007) Modulation of the receptive fields of midbrain neurons elicited by thalamic electrical stimulation through corticofugal feedback. *J Neurosci* 27: 10651–10658.
28. Lee CC, Sherman SM (2008) Synaptic properties of thalamic and intracortical inputs to layer 4 of the first- and higher-order cortical areas in the auditory and somatosensory systems. *J Neurophysiol* 100:317–326.
29. Lee CC, Sherman SM (2009) Modulator property of the intrinsic cortical projection from layer 6 to layer 4. *Front Syst Neurosci* 3:3.
30. Winer JA, Diehl JJ, Larue DT (2001) Projections of auditory cortex to the medial geniculate body of the cat. *J Comp Neurol* 430:27–55.
31. Winer JA, Larue DT, Diehl JJ, Hefti BJ (1998) Auditory cortical projections to the cat inferior colliculus. *J Comp Neurol* 400:147–174.
32. Pierret T, Lavallée P, Deschênes M (2000) Parallel streams for the relay of vibrissal information through thalamic barreloids. *J Neurosci* 20:7455–7462.
33. Kelly LR, Li J, Carden WB, Bickford ME (2003) Ultrastructure and synaptic targets of tectothalamic terminals in the cat lateral posterior nucleus. *J Comp Neurol* 464: 472–486.
34. Berman RA, Wurtz RH (2008) Exploring the pulvinar path to visual cortex. *Prog Brain Res* 171:467–473.